# Electronic Properties of $Y_2C_3$ by First-Principles Calculations

Yusuke Nishikayama, Tatsuya Shishidou and Tamio Oguchi

*Department of Quantum Matter, ADSM, Hiroshima University, Kagamiyama, Higashihiroshima, 739-8530*

The electronic and structural properties of $Y_2C_3$ are studied from first principles. We optimize all the structural parameters, the lattice constant and internal atomic positions, assuming the observed crystal structure symmetry. We also examine the lattice-constant and the C dimer bond length dependences of the electronic properties of $Y_2C_3$. It is found that there is a peak structure in close vicinity to the Fermi energy in the density of states for the optimized structure at all the lattice constants studied. This peak structure comes from a flat band along ΓN line.

KEYWORDS: $Y_2C_3$, electronic structure, Fermi surface, Fermi velocity, first-principles calculations, superconductivity

## 1. Introduction

Yttrium sesquicarbide $Y_2C_3$ has been recently found to be a superconductor with the transition temperature $T_c = 18$K,[1] which is the highest among all known binary metal carbides TaC ($T_c = 10.2$ K), WC ($T_c = 10$ K), NbC ($T_c = 11.1$ K), MoC ($T_c = 14.3$ K),[2] $YC_2$ ($T_c = 3.88$ K)[3] and $La_2C_3$ ($T_c = 11$ K ).[4,5] It has been also found that $T_c$ and the lattice constant of $Y_2C_3$ vary by high-pressure synthesis conditions.[1] In this context, lower $T_c$ (6 – 11.5K) phases with larger lattice constants were reported several decades ago.[6]

$Y_2C_3$ has bcc $Pu_2C_3$ type crystal structure (space group $I\bar{4}3d$) and contains four formula units (8 yttrium and 12 carbon atoms) in a primitive unit cell.[7] Crystallographically independent atomic positions are given at $(u, u, u)$ for Y and $(v, 0, 1/4)$ for C. This crystal structure is characterized by the existence of C dimers. However, the observed bond length of the C dimer (1.53Å)[7] is not well reproduced by a previous first-principles calculation (1.33Å).[8] Note that the theoretical bond length is rather close to that of the isolated C dimer (1.24Å).[9] Electronic structure calculations of $Y_2C_3$ have been reported by Shein and Ivanovskii[10] and Singh and Mazin.[8] Shein and Ivanovskii have calculated the electronic structure of $Y_2C_3$ and $YC_2$($T_c = 4$ K) by using the full-potential linear muffin-tin orbital (FPLMTO) method within the generalized gradient approximation (GGA) and concluded that the density of states at the Fermi energy for $Y_2C_3$ is about 37% higher than that for $YC_2$, which is a reason why $T_c$ in $Y_2C_3$ is higher than in $YC_2$. Singh and Mazin have also calculated the electronic structure of $Y_2C_3$ by the general potential linearized augmented plane wave method within the local density approximation (LDA) and discussed the charge density, the Fermi surfaces and the

electron-phonon coupling. They have claimed that the electronic structure relevant to the superconductivity is qualitatively similar to other metal carbide superconductors and not like $MgB_2$ or $A_3C_{60}$. However, information concerning the structural dependence of the electronic structure for $Y_2C_3$ is still lacking. In this paper, the structural dependences of the electronic properties of $Y_2C_3$ are investigated by first-principles calculations.

## 2. Methods

Our first-principles electronic structure calculations are based on the density functional theory[11,12] within LDA[13] and GGA.[14] One-electron Kohn-Sham equations are solved self-consistently by using our all-electron scalar-relativistic code adopting the full-potential linear augmented plane wave (FLAPW) method.[15–18] We use 20×20×20 uniform k mesh (446 points in the irreducible wedge of the Brillouin zone) with the improved tetrahedron method.[19] We assume the muffin-tin sphere radii of 1.0Å for Y and 0.65Å for C. The plane-wave basis set up to the cutoff energy of 20 Ry is utilized to expand the Kohn-Sham wave functions.

## 3. Results and Discussion

We first carried out the structural optimization with keeping the space group $I\bar{4}3d$. We took several different lattice constants, for which all atom positions ($u$ and $v$ parameters) are optimized till the largest atomic force becomes less than 5 mRy/a.u. Calculated total-energy values are fitted to the Murnaghan equation of state to find the equilibrium lattice constant and bulk modulus. Obtained lattice constant and atomic position parameters within GGA are listed in Table I. The calculated equilibrium lattice constant is 8.106Å (LDA) and 8.254Å (GGA), which is approximately 1.5 - 1.6% smaller (LDA) and 0.2 - 0.3% larger (GGA) than the experimental data 8.226Å,[1] 8.2335Å[7] and 8.2372Å.[20] The theoretical lattice constant is generally in good agreement with experiments. A seriously underestimated lattice constant ($a$ = 7.686Å) has been predicted by the previous FPLMTO calculation with GGA.[10] This may be due to unrelaxed internal atomic positions. The difference between experimental data about the C position may come from difficulty in the refinement due to sample stoichiometry.[8] The calculated equilibrium bulk modulus is 140 GPa (LDA) and 117 GPa (GGA) and the first derivative of the bulk modulus is 4.68 (LDA) and 6.74 (GGA). The nearest-neighbor C-C and Y-C distances calculated for $Y_2C_3$ as a function of the lattice constant is plotted in Fig. 1. A change in the C dimer bond length due to the variation in the lattice constant is much smaller (in a range between 1.33 – 1.34Å) than that of the nearest-neighbor Y-C distance. Thus one can say that the bonding nature in the C dimer is rather insensitive to the crystal volume. The previous theoretical calculation[8] has predicted for the experimentally determined lattice constant $a$=8.226Å the C-C and Y-C distances of 1.33Å and 2.51Å, respectively, which are in fairly good agreement with our calculated ones. The latest experimental refinement[20] has shown that the C-C and Y-C distances are 1.298 and 2.510Å, respectively. On the other hand,

it has been reported that the experimental C-C and Y-C distances are 1.53Å and 2.51Å, respectively,[7] of which the C-C distance is about 12% larger than our theoretical prediction.

Figure 2 shows total density of states (DOS) and partial DOS calculated for $Y_2C_3$ with the optimized lattice constant and atomic position parameters within GGA. By inspecting the wave functions, the main component of each valence band is composed of C-2$s\sigma^*$ between $-8$ and $-6$eV, C-2$p\sigma$ between $-6$ and $-5$eV, and C-2$p\pi$ between $-5$ and $-3$eV, relative to the Fermi energy, where a symbol (*) denotes the anti-bonding states. The Fermi energy is located in the C-2$p\pi^*$ bands hybridized with Y-4$d$ orbitals. Figure 3 shows total DOS calculated for $Y_2C_3$ with the lattice constants of $a$ = 8.1, 8.2, 8.3 and 8.4Å, where all atomic positions are fully optimized. It is noted that there is a peak structure in close vicinity to the Fermi energy in DOS for all the lattice constants studied. The peak comes from the C-2$p\pi^*$ and Y-4$d$ hybridization. The existence of the peak at the Fermi energy in DOS favors raising $T_c$. Figure 4 shows total and partial DOS calculated for $Y_2C_3$ with the experimental crystal structure,[7] which is characterized by the C dimers with a longer bond length (1.53Å). Note that there is no peak in close vicinity to the Fermi energy in DOS at all. We compare our result with the previous theoretical ones.[8,10] Our calculated total DOS for $Y_2C_3$ in Fig. 2 agrees well with the previous ones. The peak structure in close vicinity to the Fermi energy in the total DOS is also seen.

The lattice-constant dependence of the calculated total DOS at the Fermi energy for $Y_2C_3$ is plotted in Fig. 5. It can be seen that the total DOS decrease as the lattice constant increases between 8.0 and 8.5Å. Thus we can say that Tc might increase if the pressure is added. The calculated bare linear specific heat coefficient calculated for $Y_2C_3$ with the optimized crystal structure within GGA is $\gamma$ = 4.55 mJ/mol K$^2$, which is approximately 24% smaller than experimental data 6.0 mJ/mol K$^2$ .[21] Our calculated specific heat coefficient is slightly larger than the other theoretical specific heat coefficient 4.4 mJ/mol K$^2$ [8] with the lattice constant of $a$ = 8.226Å and the internal atomic structures relaxed. We discuss the origin of the peak appearing at the Fermi energy in DOS when distance between the C atoms is short. There is a peak structure in close vicinity to the Fermi energy in DOS for the optimized structure at all lattice constants studied, while there is no such peak for the reported structure with C dimer bond length of 1.53Å.[7] Then a change in the dimer bond length due to the variation in the lattice constant is small. Thus we can say that C dimer bonding is important for the peak at the Fermi energy.

Figure 6 shows band structure calculated for $Y_2C_3$ with the optimized crystal structure within GGA. It is quite interesting that there is a flat band on the ΓN line. This is also the case for all the lattice constants studied. Figure 7 shows band structure calculated for $Y_2C_3$ with the experimental crystal structure with longer C dimer bond (1.53Å). We see that there is no such a flat-band feature on the ΓN line. Figure 8 shows the band structure of $Y_2C_3$

with shorter C dimer bond (1.34Å) along (a) Γ N ([110]), (b) [001] and (c) [1$\bar{1}$0] lines passing through the point (0.25, 0.25, 0). The band crossing the Fermi energy is upward convex along [110] while downward convex along [1$\bar{1}$0] and [001]. Therefore, the point (0.25, 0.25, 0) is a saddle point. So we can say that the peak structure in close vicinity to the Fermi energy in the density of states comes from this saddle-point feature on the ΓN line.

The band structure calculated for $Y_2C_3$ with the optimized crystal structure within GGA is fitted with symmetrized star functions[22] by a spline method and used for calculations of the Fermi surface, the Fermi velocity, and the Hall coefficients of $Y_2C_3$. Figure 10 shows the Fermi surface of $Y_2C_3$. There are four kinds of Fermi surfaces, three of which are hole surfaces and the other is electron one. We note that a horn-like shape directed to N in (d) of Fig. 10 comes from the intersection between the flat band on the ΓN line and Fermi energy near N. The calculated Fermi velocity of $Y_2C_3$ is $< v^2 >^{1/2} = 1.6\times10^7$ cm/s. We show calculated Fermi velocities of some superconductors for comparison in Table II. The Fermi velocities in $MgB_2$, $La_{1.85}Sr_{0.15}CuO_4$ and $YBa_2Cu_3O_7$ show anisotropy, which comes from anisotropy of the crystal structure, while the Fermi velocity in $Y_2C_3$ is isotropic because of cubic structure. The Fermi velocity in $Y_2C_3$ is the same order of magnitude but smaller than that of $MgB_2$, $La_{1.85}Sr_{0.15}CuO_4$ and $YBa_2Cu_3O_7$. The Fermi velocity can be decomposed into components of bands that make Fermi surfaces. Each component is shown in Table III. We notes that the magnitude of Fermi velocities of hole band 1, 2, 3 are large compared with one of electron band 4. It may be related to the fact that $Y_2C_3$ is a multigap superconductor.[25] The Hall coefficient in $Y_2C_3$ is also estimated to be $+1.6\times10^{-9}$ m$^3$/C. The positive sign of the Hall coefficient means that the dominant carrier is a hole. It is strongly desired to carry out transport experiments such as Hall measurement. Superconductors without inversion symmetry are investigated using effect of the spin-orbit interaction[26,27] and $Y_2C_3$ has no inversion symmetry. Thus it is important to know effect of the spin-orbit interaction in $Y_2C_3$. We include the spin-orbit interaction (SOI) as the second variation every self-consistent-field step. In the second-variation procedure, states up to 25.4 eV above $\epsilon_F$ are included. The $\boldsymbol{k}$ states with different spin that cross the Fermi energy split by 0.009 to 0.015 eV along ΓP line and 0.002 to 0.013 eV along ΓN line by SOI. It is reported that the SOI band splitting of $CePt_3Si$ is of the order of 0.05 to 0.2 eV. Thus we can say that the SOI band splitting of $Y_2C_3$ is an order of magnitude smaller than that of $CePt_3Si$ .[28]

## 4. Conclusion

The electronic properties of $Y_2C_3$ are investigated based on first-principles calculations. The optimized C-C bond length is 1.34Å, which is much shorter than that obtained experimentally, and the crucial factor to determine the electronic structure near the Fermi energy. It is characteristic that there is a peak structure in close vicinity to the Fermi energy in the total DOS for the optimized structure at all lattice constants studied. The peak originates in

the C-2$p\pi^*$ and Y-4$d$ hybridization. we have found that the peak structure in close vicinity to the Fermi energy in the density of states comes from a saddle point on ΓN line in the Brillouin zone.

**Acknowledgments**

The authors would like to thank J. Akimitsu and S. Akutagawa for invaluable discussion. The numerical computation was performed on the Supercomputing Facilities at the Institute for Solid State Physics, University of Tokyo.

## References


1) G. Amano, S. Akutagawa, T. Muranaka, Y. Zenitani and J. Akimitsu: J. Phys. Soc. Jpn. **73** (2004) 530.
2) C. P. Poople, Jr.: Handbook of Superconductivity (Academic Press, San Diego, 2000).
3) A. L. Giorgi, E. G. Szklarz, M. C. Krupka, T. C. Wallace and N. H. Krikorian: J. Less-Common Met. **14** (1968) 247.
4) A. L. Giorgi, E. G. Sklarz, M. C. Krupka and N. H. Krikorian: J. Less-Common Met. **17** (1969) 121.
5) A. L. Giorgi, E. G. Sklarz, N. H. Krikorian and M. C. Krupka: J. Less-Common Met. **22** (1970) 131.
6) M. C. Krupka, A. L. Giorgi, N. H. Krikorian and E. G. Szklarz: J. Less-Common Met. **17** (1969) 91.
7) V. I. Novokshonov: Russian J. Inorganic Chem. **25** (3) (1980) 375.
8) D. J. Singh and I. I. Mazin: Phys. Rev. B **70** (2004) 052504 ; The internal parameter u=0.504 seems to be a mistake and the correct one should be u=0.0504.
9) K. P. Huber and G. Herzberg: Molecular Spectra and Molecular Structure. IV Constants of Diatomic Molecules (Van Nostrand Reinhold, New York, 1979).
10) I. R. Shein and A. L. Ivanovskii: Solid State Commun. **131** (2004) 223.
11) P. Hohenberg and W. Kohn: Phys. Rev. **136** (1964) B864.
12) W. Kohn and L. J. Sham: Phys. Rev. **140** (1965) A1133.
13) J. F. Janak, V. L. Moruzzi and A. R. Williams: Phys. Rev. B **12** (1975) 1257.
14) J. P. Perdew, K. Burke and M. Ernzerhof: Phys. Rev. Lett. **77** (1996) 3865.
15) E. Wimmer, H. Krakauer, M. Weinert and A. J. Freeman: Phys. Rev. B **24** (1981) 864.
16) M. Weinert, E. Wimmer and A. J. Freeman: Phys. Rev. B **26** (1982) 4571.
17) H. J. F. Jansen and A. J. Freeman: Phys. Rev. B **30** (1984) 561.
18) J. M. Soler and A. R. Williams: Phys. Rev. B **40** (1989) 1560.
19) P. E. Blöchl, O. Jepsen and O. K. Andersen: Phys. Rev. B **49** (1994) 16223.
20) T. Mochiku, T. Nakane, H. Kito, H. Takeya, S. Harjo, T. Ishigaki, T. Kamiyama, T. Wada and K. Hirata: Physica C **426-431** (2005) 421.
21) S. Akutagawa and J. Akimitsu: J. Phys. Soc. Jpn. **76** (2007) 024713.
22) W. E. Pickett, H. Krakauer and P. B. Allen: Phys. Rev. B **38** (1988) 2721.
23) J. Kortus, I. I. Mazin, K. D. Belashchenko, V. P. Antropov and L. L. Boyer: Phys. Rev. Lett. **86** (2001) 4656.
24) P. B. Allen, W. E. Pickett and H. Krakauer: Phys. Rev. B **37** (1988) 7482.
25) A. Harada, S. Akutagawa, Y. Miyamichi, H. Mukuda, Y. Kitaoka and J. Akimitsu: cond-mat/0612578.
26) P. A. Frigeri, D. F. Agterberg, A. Koga and M. Sigrist: Phys. Rev. Lett. **92** (2004) 097001.
27) S. Fujimoto: cond-mat/0605290.
28) K. V. Samokhin, E. S. Zijlstra and S. K. Bose: Phys. Rev. B **69** (2004) 094514.

Table I. Calculated lattice constant $a$ in Å and atomic position parameters $u$ and $v$ within GGA.

| | $u$ | $v$ | $a$ |
|---|---|---|---|
| Present work | 0.0500 | 0.2936 | 8.254 |
| Theory[8)] | 0.0504 | 0.2940 | 8.226* |
| Experiment[1)] | | | 8.226 |
| Experiment[7)] | 0.05 | 0.2821 | 8.2335 |
| Experiment[20)] | 0.0505 | 0.2962 | 8.2372 |

*): Lattice constant was fixed to the observed one.[1)]

Table II. Calculated Fermi velocities ($10^7$ cm/s).

| | $< v_x^2 >^{1/2}$ | $< v_y^2 >^{1/2}$ | $< v_z^2 >^{1/2}$ | $< v^2 >^{1/2}$ | Crystal system |
|---|---|---|---|---|---|
| $Y_2C_3$ (Present work) | 0.95 | 0.95 | 0.95 | 1.64 | Cubic |
| $MgB_2$ ([23]) | 4.90 | 4.90 | 4.76 | 8.41 | Hexagonal |
| $La_{1.85}Sr_{0.15}CuO_4$ ([24]) | 2.2 | 2.2 | 0.41 | 3.14 | Tetragonal |
| $YBa_2Cu_3O_7$ ([24]) | 1.8 | 2.8 | 0.7 | 3.40 | Orthorhombic |

Table III. Calculated total DOS at the Fermi energy and calculated Fermi velocities decomposed into components of bands that make Fermi surfaces. Bands 1, 2, 3 and 4 correspond to the Fermi surface of (a), (b), (c) and (d) in Fig. 10, respectively.

| | band 1 | band 2 | band 3 | band 4 | total |
|---|---|---|---|---|---|
| $D(\epsilon_{\rm F})$ (/eV unit cell spin) | 0.12 | 0.15 | 0.88 | 2.73 | 3.88 |
| $< v^2 >^{1/2}$ ($10^7$ cm/s) | 2.54 | 2.58 | 2.12 | 1.31 | 1.64 |

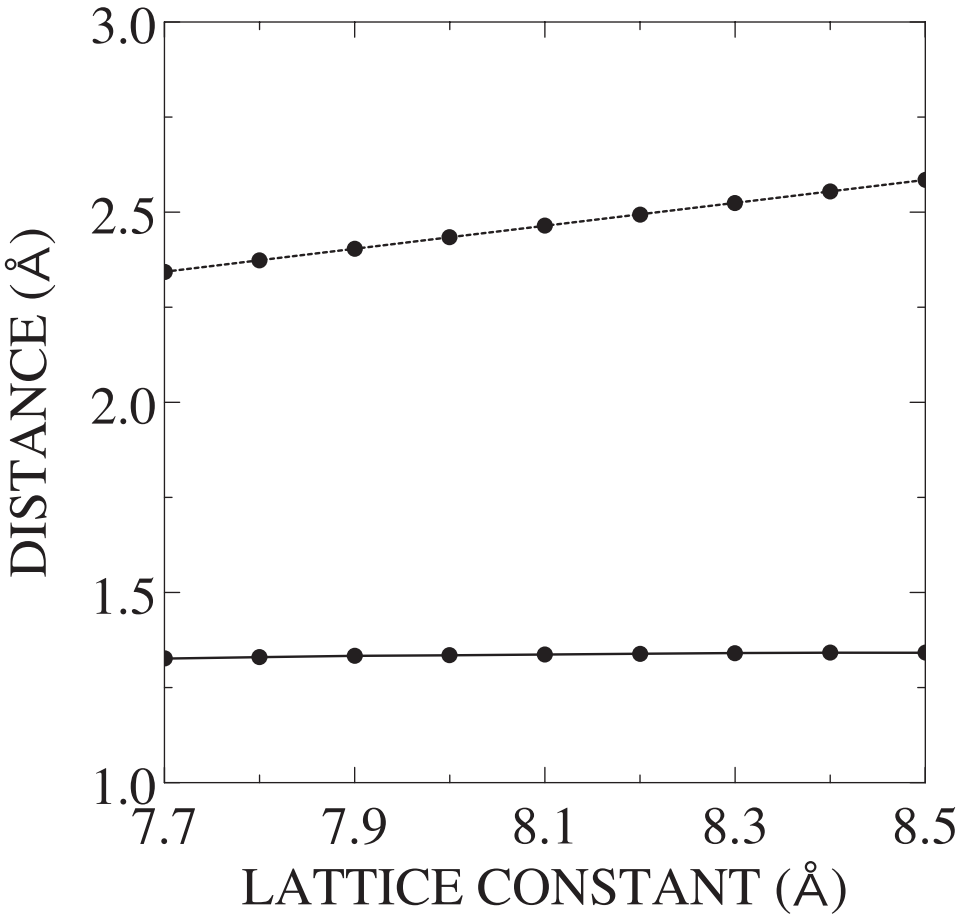


Fig. 1. The upper and lower lines show the nearest-neighbor Y-C and C-C distances, respectively.

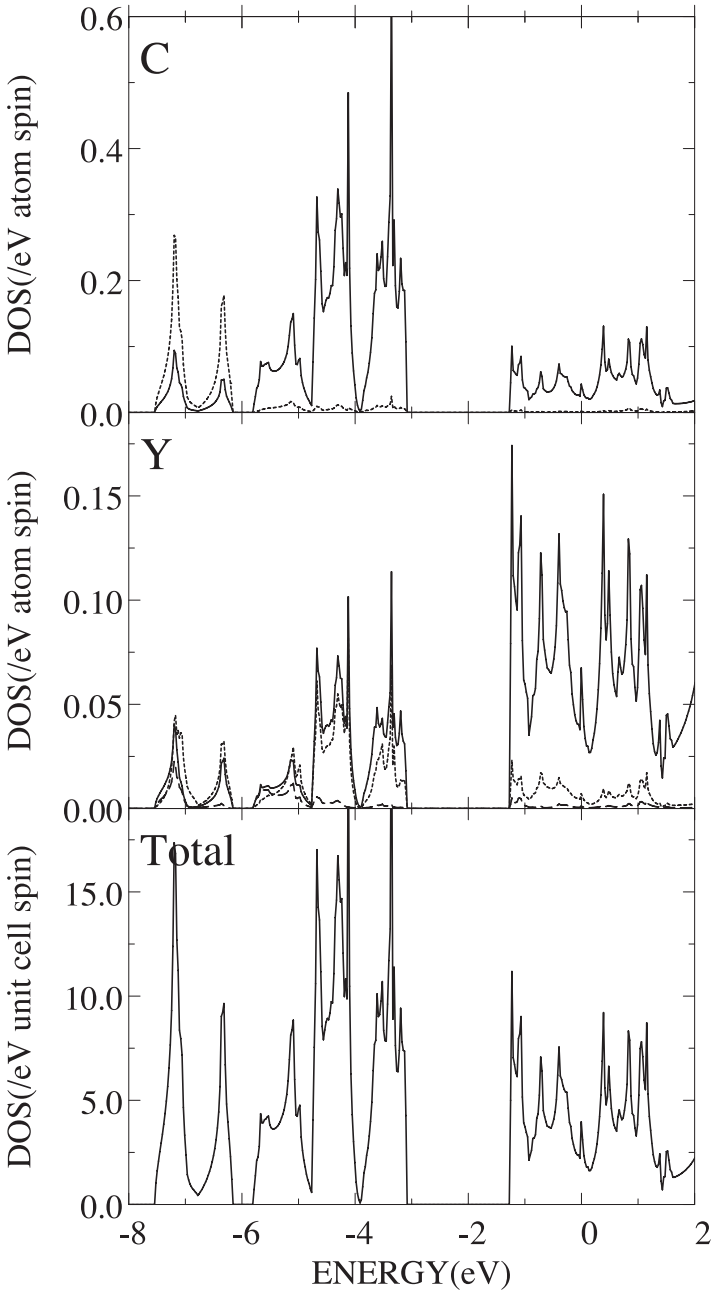


Fig. 2. Total and partial density of states calculated for $Y_2C_3$ with the optimized crystal structure within GGA. As for the partial density of states for Y, dashed, dotted and solid lines denotes s, p and d components, respectively. As for ones for C, dotted and solid lines denotes s and p components, respectively. The Fermi energy is set to the origin.

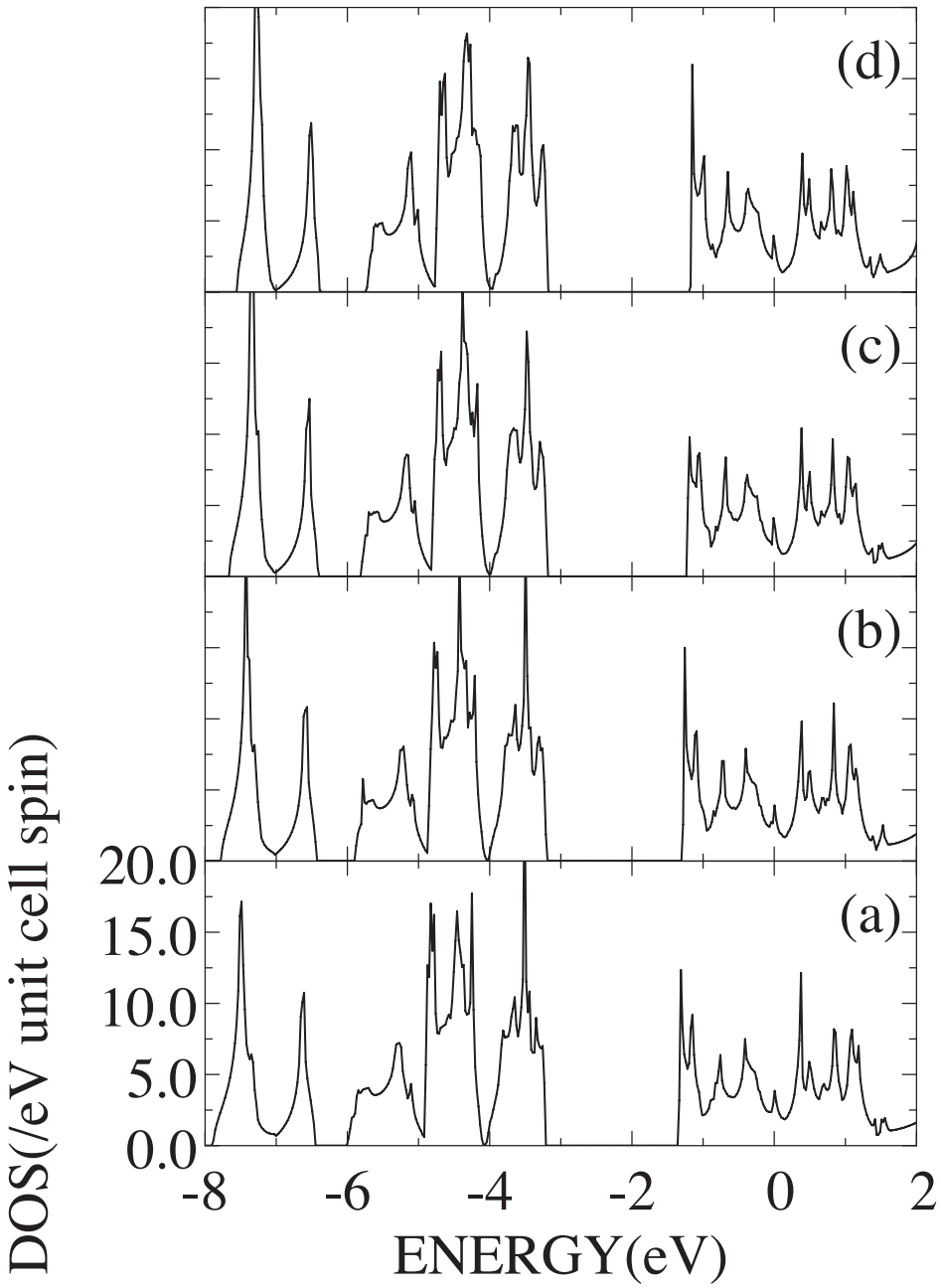


Fig. 3. Total density of states calculated for $Y_2C_3$ with different lattice constant $a$ = 8.1 - 8.4Å. (a) $a$=8.1Å, (b) $a$=8.2Å, (c) $a$=8.3Å and (d) $a$=8.4Å. The Fermi energy is set to the origin.

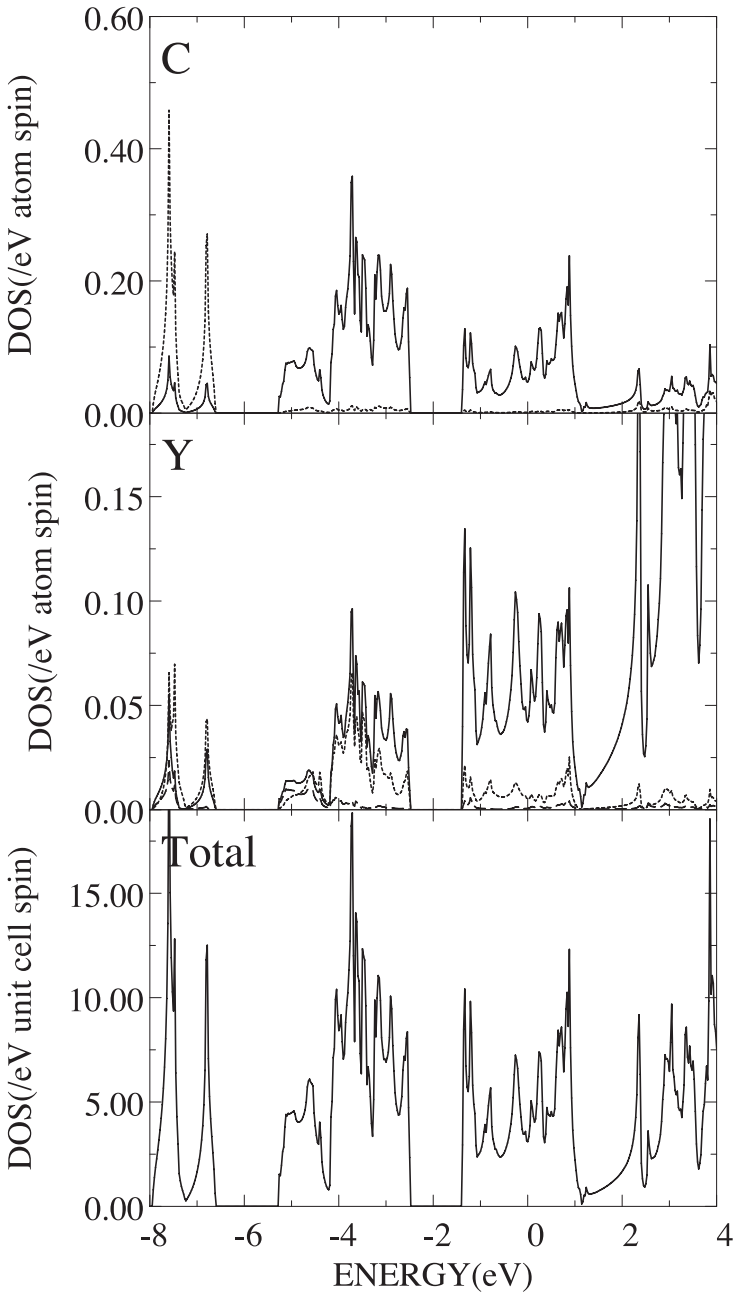


Fig. 4. Total density of states and partial density of states calculated for $Y_2C_3$ with the experimental crystal structure with longer C dimer bond (1.53Å).[7] As for the partial density of states for Y, dashed, dotted and solid lines denotes s, p and d components, respectively. As for ones for C, dotted and solid lines denotes s and p components, respectively. The Fermi energy is set to the origin.

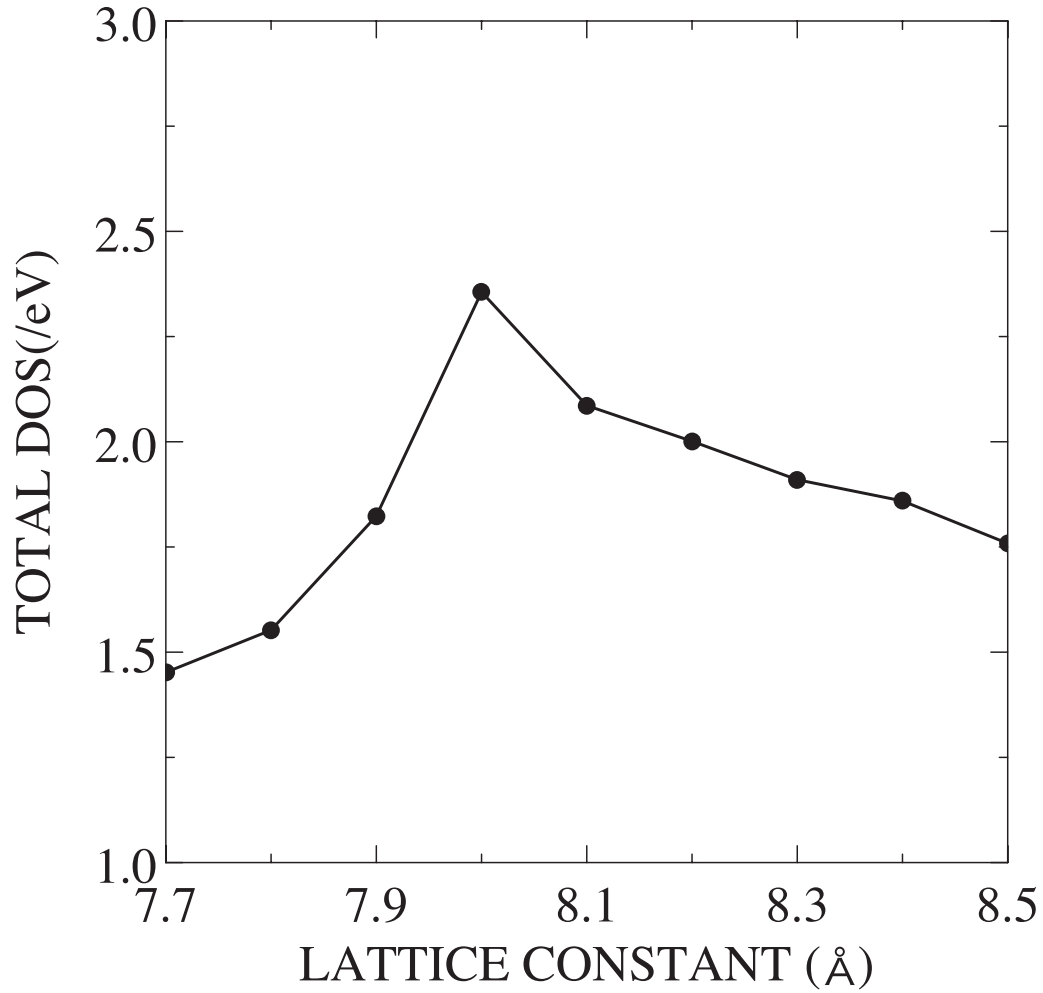


Fig. 5. The lattice-constant dependence of the calculated total DOS at the Fermi energy for $Y_2C_3$ in states/eV-f.u.

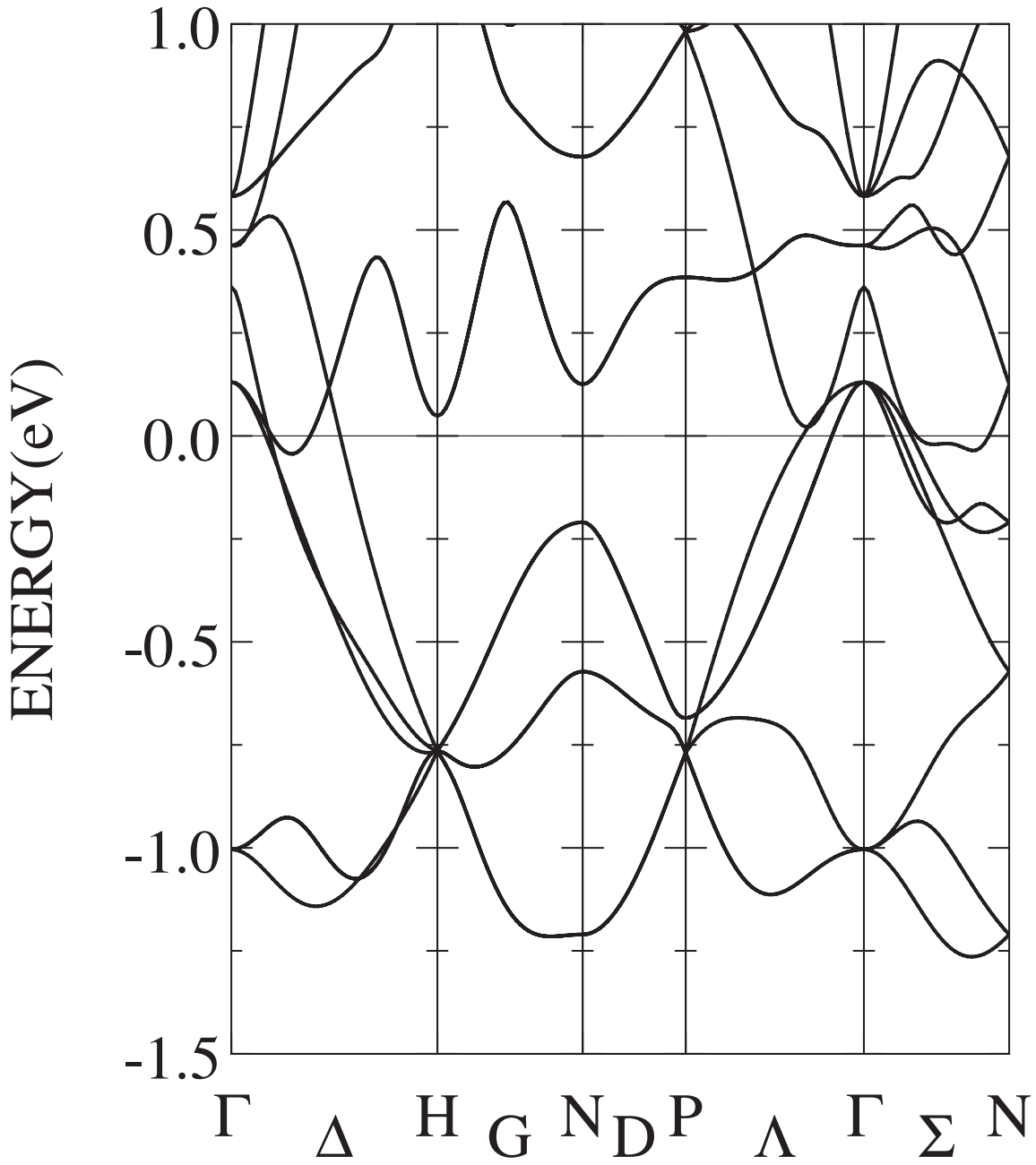


Fig. 6. Calculated energy band structure of $Y_2C_3$ with the optimized crystal structure within GGA along high-symmetry lines. The Fermi energy is set to the origin.

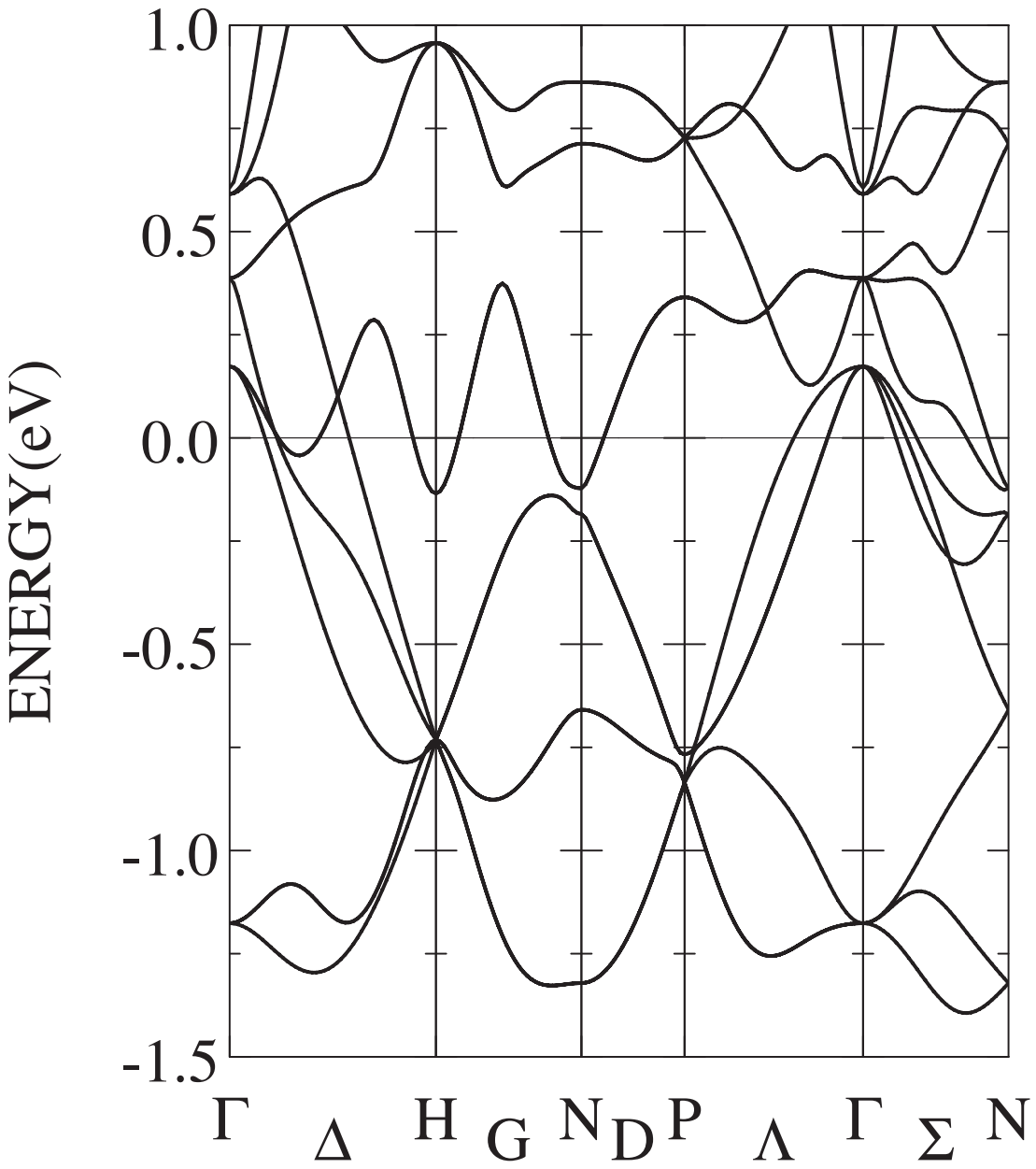


Fig. 7. Calculated energy band structure of $Y_2C_3$ with the experimental crystal structure with longer C dimer bond (1.53Å)[7] along high-symmetry lines. The Fermi energy is set to the origin.

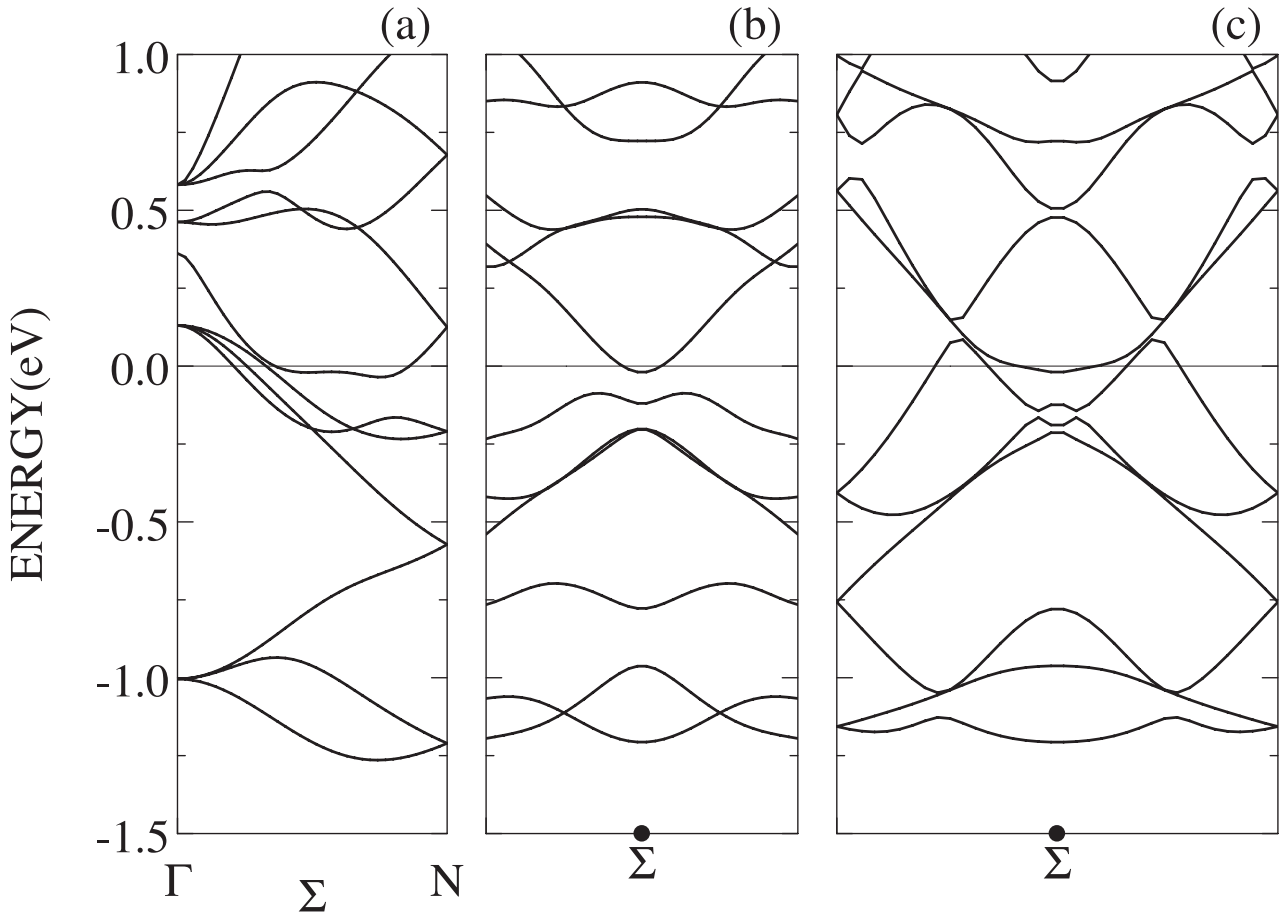


Fig. 8. Calculated energy band structures of $Y_2C_3$ with shorter C dimer bond (1.34Å) along (a) Γ(0, 0, 0) - N($\frac{1}{2}$, $\frac{1}{2}$, 0), (b) ($\frac{1}{4}$, $\frac{1}{4}$, $\frac{1}{2}$) - ($\frac{1}{4}$, $\frac{1}{4}$, -$\frac{1}{2}$) and (c) ($\frac{3}{4}$, -$\frac{1}{4}$, 0) - (-$\frac{1}{4}$, $\frac{3}{4}$, 0).

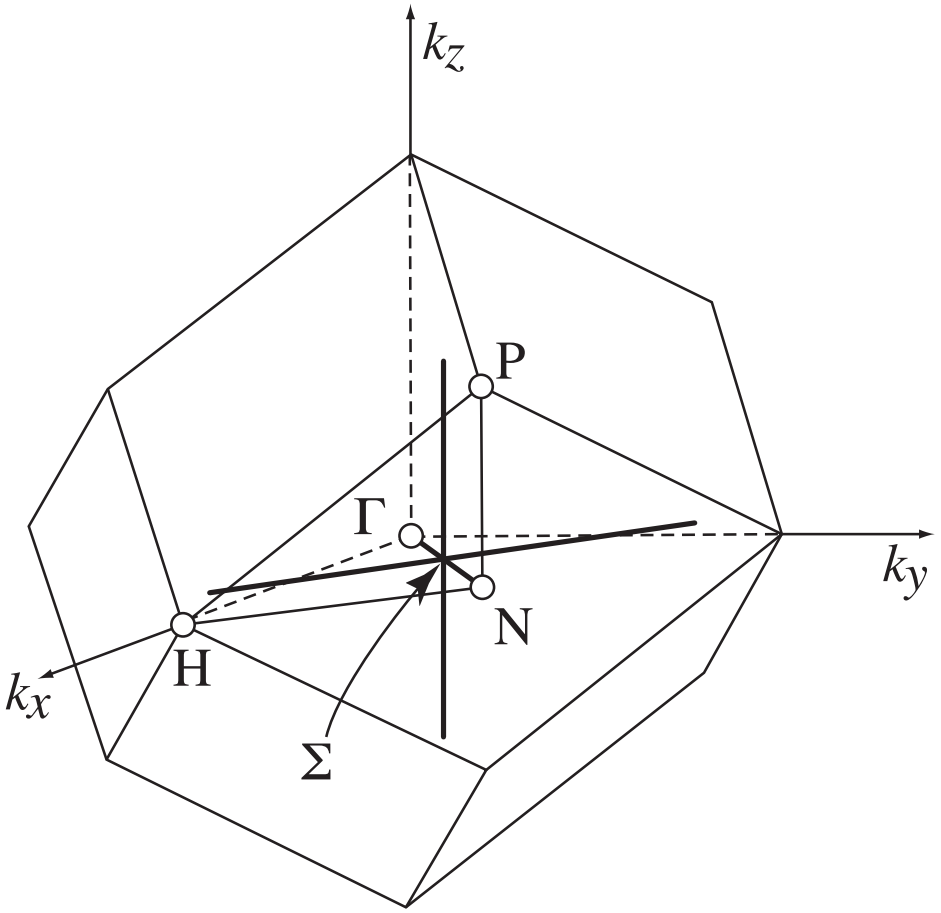


Fig. 9. Three k-point lines in the Brillouin zone on which the band structure is drawn in Fig. 8. The cross point of the lines is Σ.

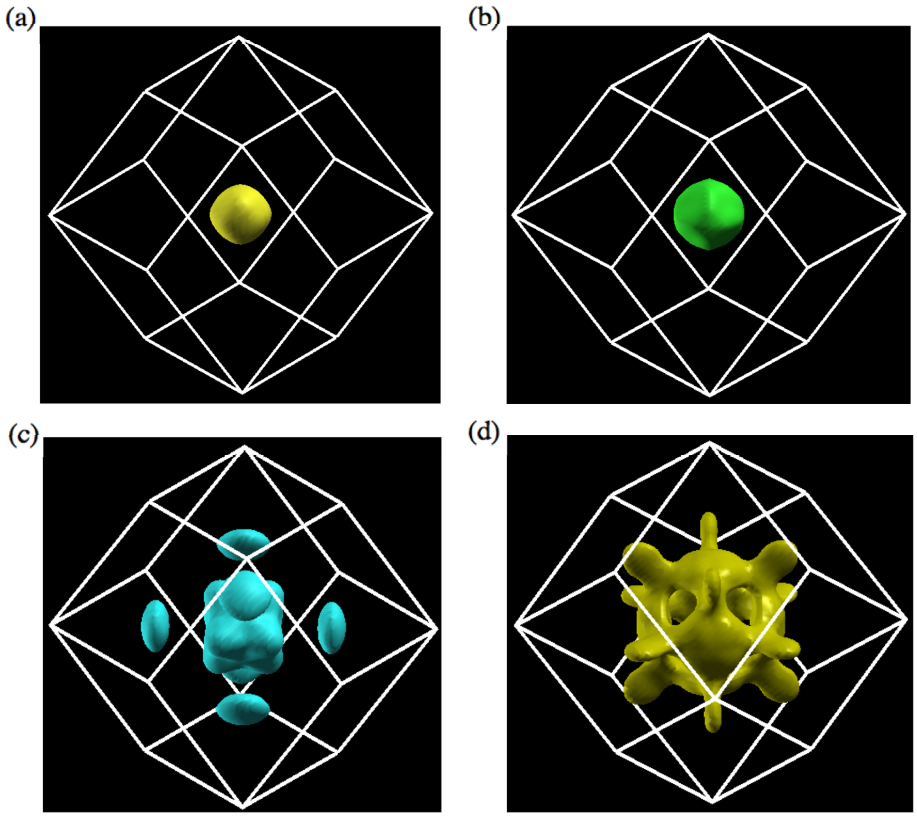


Fig. 10. (Color online) Calculated Fermi surfaces of $Y_2C_3$: (a), (b), and (c) hole surfaces and (d) electron surface. The  point is placed at the center of the bcc Brillouin zone.